Latin American Journal of Solids and Structures
www.lajss.org

Numerical Study of Vibro-Acoustic Responses of Un-Baffled Multi-Layered Composite Structure under Various End Conditions and Experimental Validation

Abstract

This article presents the vibro-acoustic modeling and analysis of un-baffled laminated composite flat panels subjected to harmonic point load under various support conditions. The frequency values of the panel are obtained by using simulation model through the commercial finite element package (ANSYS) via batch input technique. Initially, the rate of convergence of the current simulation results is established by solving different examples under various edge supports. Further, the natural frequencies and corresponding modes are computed and compared with available published and experimentally obtained values. Then, the modal values are exported to LMS Virtual.Lab environment for the computation of acoustic responses of the vibrating laminated plate structure. Further, an indirect boundary element approach has been adopted to extract the coupled vibro-acoustic responses. Subsequently, the radiated sound power of the structure and the sound pressure level within the acoustic medium are computed using the present scheme and compared with the published numerical results and in-house experimental data, respectively. Finally, a comprehensive study has been performed to highlight the effect of different structural parameters (thickness ratio, aspect ratio, modular ratio and lay-up scheme), support conditions and the composite properties on the acoustic radiation responses of the laminated plate structure.

Keywords

Laminated composite; Modal analysis; Indirect boundary element method; SPL; Radiated sound power; Experimental analysis.

Nitin Sharma [a]
Trupti Ranjan Mahapatra [b]
Subrata Kumar Panda [c]

[a] Ph.D Stu., Sch. of Mech. Engineering, KIIT University, Bhubaneswar, Odisha, India, nits.iiit@gmail.com
[b] Assoc. Prof., Sch. of Mech. Eng., KIIT University, Bhubaneswar, Odisha, India, trmahapatrafme@kiit.ac.in
truptiranjan01@gmail.com
[c] Asst. Prof., Dept. of Mech. Eng., NIT, Rourkela, Odisha, India, call2subrat@gmail.com

http://dx.doi.org/10.1590/1679-78253830

Received 14.03.2017
In revised form 27.04.2017
Accepted 14.06.2017
Available online 17.06.2017

1 INTRODUCTION

Laminated composite structural components are extensively preferred over conventional materials in today's high-performance engineering applications (aerospace, aircraft, automobile and marine engi-

neering) not only for their specific strength and stiffness properties but also largely due to their light weight characteristic which is highly desirable according to the present demand. However, the reduction in weight of the structure may lead to increased levels of noise which is proportional to the magnitude and frequency of the structural vibrations. Therefore, the designer quest to minimize the noise radiated into the surroundings during the design and fabrication of the light-weight laminated structural components due to their paramount importance in such applications. Hence, the sound radiation characteristics need to be investigated judiciously and the design together with the fabrication process must be handled suitably. It is well known that, a radiation response indicator is essential for the representation of the acoustic radiation via a vibrating structure so that the velocity on the boundary and the sound radiation can be related. Thus, it plays an important role in the evaluation of the magnitude of the acoustic disturbances accurately. In this regard, various acoustic radiation mode theories including the structure dependent radiation mode analysis steps have been evolved in the past with an intention to figure out the realistic acoustic radiation in the surrounding medium due to the vibrating structures (baffled and un-baffled plates and beams) (Atalla and Sgard, 2015). The acoustic radiation of the flat rectangular plate in a rigid baffle is usually obtained by Rayleigh integral formulation and often used as the basis for the analysis of sound radiation analysis for more complex structures. This scheme is further extended by other researchers successively in the past to explore the possible effect of angle of the baffle and the end constraint conditions on the acoustic radiation behaviour (Putra and Thompson, 2010). The first radiation mode amplitude of the composite and the isotropic plate structures have frequently been employed to account the acoustic behaviour (Petrone et al., 2014). However, so far as the analysis of laminated and sandwich structures is concerned, the existing and/or refined 2D and shear deformation theories are mainly employed to obtain the vibration responses of the structure and the acoustic radiation is computed using Rayleigh integral (Petrone et al., 2014). However, we also note that, in those studies the use of structure dependent radiation modes is preferred over the conventional acoustic radiation modes to quantify the acoustic radiation from the vibrating structures (Ohlrich and Hugin, 2004).

Another aspect related to the study of the vibro-acoustic responses of any structure for which the methodologies have been modified from time to time is to solve the multi-physics problems (fluid-structural coupling). The core idea is to establish a coupling between the free vibration response of the structures and the acoustic medium more accurately. Atalla et al. (1996) studied the acoustic radiation from un-baffled thin flat isotropic structures using Rayleigh-Ritz approximation for acoustic parameters and compared the results to the baffled case. A modal superposition technique has been utilised for the computation of coupled structure and acoustic modes by Tournour and Atalla (1998) including a novel integration scheme proposed for handling the singularities of Green's function. Attempts have also been made frequently to investigate the vibro-acoustic responses of structures using the finite element method (FEM) in association with boundary element method (BEM) (Everstine and Henderson, 1990) to analyse the coupled behaviour. Holmstrom (2001) used a direct FEM/BEM approach to account for the acoustic radiation from an elastic plate vibrating in air and water under harmonic pressure excitation. In the similar line, Li and Li (2008) studied the effects of size and location of distributed mass loading on the acoustic radiation from the baffled plates vibrating in light and heavy medium. Jeyaraj and his colleagues investigated the vibro-acoustic response of isotropic plates (2008) and fiber reinforced composite plates (2009) under thermal envi-

ronment. The classical laminated plate theory (CLPT) has been used to model the structure and the acoustic response is obtained using coupled FEM/BEM solver in LMS SYSNOISE software. Yin and Cui (2009) studied the effect of the lay-up scheme on the acoustic behaviour of laminated composite plates under different loading schemes, namely transverse and longitudinal. Acoustic radiation from a functionally graded (FG) elliptic disc in a thermal environment has been studied by Kumar et al. (2009) by using FEM/BEM approach and LMS SYSNOISE software. Zhao et al. (2013) considered a simply supported laminated composite flat plate vibrating in a hygroscopic environment and obtained the acoustic response by using Rayleigh integral formulation. Nowak and Zielinski (2015) used an indirect variational BEM to get the acoustic radiation from vibrating rectangular plate for various boundary conditions. The frequencies and the corresponding vibrational mode shapes of the plate are computed using the FEM. The effect of support conditions on the velocity and acoustic response of vibrating rectangular isotropic baffled plates has also been studied using Rayleigh integral formulation (Park et al., 2003; Qiao and Huang, 2007). The support tuning is observed to yield significant noise and vibration reduction. Huang et al. (2005) investigated the free vibration behaviour of orthotropic rectangular plates with varying thickness under general boundary conditions. Shojaeefard et al. (2014) presented an analytical solution for calculating the sound transmission loss of thick orthotropic cylindrical shell using third order shear deformation theory (TSDT).

It is clear from the brief review of the literature that the boundary conditions, along with the other parameters such as type of excitation, location of excitation, material properties etc. play an important role in determining the acoustic radiation behaviour of structures. We also note that the studies related to the vibro-acoustic response of baffled isotropic plates are more in number in comparison to the baffled and/or un-baffled laminated composite structures. However, theoretical and numerical studies addressing the effect of frequently used support conditions on the acoustic radiation characteristics of an un-baffled orthotropic laminated composite flat panel under the action of harmonic point loads are scarce. In order to address this issue, in this paper an attempt has been made to study the sound radiation characteristic of the un-baffled laminated composite flat panels under several support conditions and subjected to harmonic point excitation. First, a simulation model for the vibrating flat panel has been developed in commercial FE software ANSYS using ANSYS parametric design language (APDL) code and the natural frequencies are computed. Then, these free vibration responses have been utilised to carry out the coupled vibro-acoustic analysis via indirect BEM method in LMS Virtual.Lab environment. In order to validate the proposed scheme, the present results are compared with the numerical data available in open literature. Further, lab scale experiments have been conducted to obtain the free vibration and the acoustic responses of the laminated composite plates and compared with the current numerical results. Finally, the effect of aspect ratio, thickness ratio, modular ratio and the lamination scheme on the acoustic radiation characteristics (sound pressure level and radiated sound power) of an un-baffled laminated composite flat panel under different support conditions have been investigated and discussed in detail.

2 THEORETICAL BACKGROUND

The geometry and lay-up scheme of a typical laminated composite flat panel considered for the present analysis is shown in Figure 1. It consists of N number of equally thick orthotropic layers of

length a, width b and thickness h. In order to compute the free vibration responses, a simulation model of the flat panel has been developed in ANSYS environment using APDL code. The Shell 281 element has been chosen from the ANSYS element library for the discretization of the present model. The element is a serendipity (eight noded) element with six degrees freedom per node and capable of solving thin to moderately thick shell panel structure. The mid-plane kinematic for the panel structure is defined based on the first order shear deformation theory (FSDT) and conceded as:

$$\begin{aligned} u\left(x,y,z,t\right) &= u_0\left(x,y\right) + z\theta_x\left(x,y\right) \\ v\left(x,y,z,t\right) &= v_0\left(x,y\right) + z\theta_y\left(x,y\right) \\ w\left(x,y,z,t\right) &= w_0\left(x,y\right) + z\theta_z\left(x,y\right) \end{aligned} \tag{1}$$

where, u, v and w are the displacements of any point on the Kth layer of the composite lamina at time "t" along the x, y and z coordinate axes, respectively; u_0, v_0 and w_0 are the corresponding displacements of a point on the mid-plane; θ_x and θ_y are the rotations of normal to the mid-surface ($z = 0$) about the y and x axes, respectively; θ_z is the higher order term in the Taylor series expansion which accounts for the linear variation of displacement function along thickness direction.

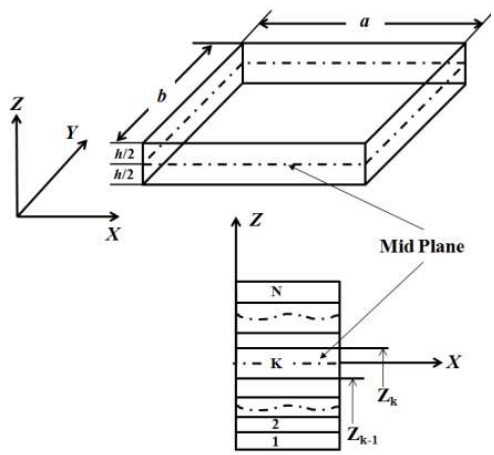

Figure 1: Geometry and lay-up scheme of laminated composite flat panel.

Now, this simulation model has been employed to perform the modal analysis as well as extract the necessary modal values of the structure. Further, the values are provided as the input for the acoustic analysis. The in-vacuo modes of the vibrating structure can be obtained by solving the following eigenvalue equation (Cook et al., 2000):

$$\left([K]-\omega^2[M]\right)\left\{\Phi\right\} = 0 \tag{2}$$

where, $[K]$ and $[M]$ are the stiffness and mass matrices, respectively, ω is the natural frequency of vibration, and $\{\Phi\}$ is the corresponding mode shape vector. The mode shapes corresponding to each natural frequency of vibration are extracted.

It is apparent from the review of literature that the BEM has been widely appreciated for solving the coupled vibro-acoustics problems efficiently. In the present study the indirect BEM has been used for modelling the fluid medium and the sound radiation is computed on both sides of the mesh. For the theoretical development an un-baffled vibrating flat panel having fluid on both of its sides is considered as shown in Figure 2. The governing equation for the acoustic problems is the well-known Helmholtz wave equation which is expressed as:

$$\nabla^2 p + k^2 p = 0 \text{ in the fluid medium } D. \tag{3}$$

where, ∇^2 is the laplacian, $k = \omega/c$ is the wave number, p is the acoustic pressure, ω is the angular frequency, c is the speed of sound in the surrounding acoustic medium (D) and S^+ and S^- denote the two separate sides of the surface S such that $S = S^+ \cup S^-$.

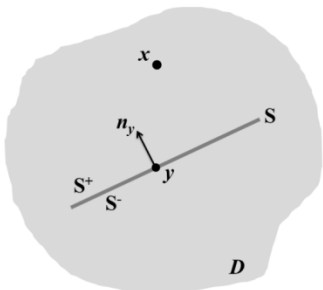

Figure 2: Un-baffled flat panel in acoustic medium.

The indirect BEM method involves the modelling of acoustic variables in the form of potentials, namely the single layer potential σ and the double layer potential μ. These potentials are related to the acoustic pressure and velocity jumps across the surface S as:

$$\sigma = \frac{\partial p^+}{\partial n} - \frac{\partial p^-}{\partial n} \tag{4}$$

and,

$$\mu = p^+ - p^- \tag{5}$$

where, superscript '+' indicates the values on the positive side defined by the outward normal vector at the surface S^+, and the superscript '−' indicates values on the opposite side, *i.e.* S^-. Now, using the potentials defined in the aforementioned lines, the solution to the Helmholtz wave equation takes the following form as in (Nowak and Zielinski, 2015):

$$p_x = -\int_S [G_{xy}\sigma_y - \frac{\partial G_{xy}}{\partial n_y}\mu_y] dS_y \text{ , } \forall x \notin S \text{ and } y \in S \tag{6}$$

where, G is the free space Green's function defined as:

$$G_{xy} = \frac{1}{4\pi r} e^{-jkr} \tag{7}$$

where, r is the distance between the source point y and the field point x.

Now, Eq. (3) is solved by imposing Neumann boundary condition on the entire surface S of the vibrating flat panel given as:

$$\sigma = 0 \text{, and } \left.\frac{\partial p}{\partial n}\right|_y = -j\omega\rho V_n \quad \text{for } y \in S \tag{8}$$

where, V_n is the normal component of velocity of the structure. On imposing the boundary condition given by Eq. (8), Eq. (6) can be re-written as:

$$-j\omega\rho V_n = \int_S \mu_y \frac{\partial^2 G_{xy}}{\partial n_x \partial n_y} dS_y \tag{9}$$

Now, Eq. (9) needs to be solved for an unknown potential μ defined on the surface S. The solution to the integral equation can be obtained by minimizing the functional J defined as in (Qiao and Huang, 2007):

$$J = 2\int_S j\omega\rho\mu_x V_{n,y} + \int_S \int_S \mu_x \mu_y \frac{\partial^2 G_{xy}}{\partial n_x \partial n_y} dS_x dS_y \tag{10}$$

Subsequently, Eq. (10) is rewritten by using the properties of Green's function G and the continuity of μ over S (Tournour and Atalla, 1998):

$$\left.\begin{aligned} \int_S \int_S \mu_x \mu_y \frac{\partial^2 G_{xy}}{\partial n_x \partial n_y} dS_x dS_y &= \int_S \int_S G_{xy}[k^2 \mu_x \mu_y (n_x \cdot n_y) - (\nabla \times \mu_x) \cdot (\nabla \times \mu_y)] dS_x dS_y \\ &= \langle \mu \rangle [D(\omega)] \{\mu\} \end{aligned}\right\} \tag{11}$$

And

$$\int_S j\omega\rho\mu_x V_{n,y} = \langle U \rangle [C] \{\mu\} \tag{12}$$

where, U is the degree of freedom vector of the structure. Therefore, a coupled equation representing the structure and acoustic medium can be written as:

$$\begin{pmatrix} K + i\omega\Theta - \omega^2 M & C \\ C^T & -\dfrac{1}{\rho\omega^2} D(\omega) \end{pmatrix} \begin{Bmatrix} U \\ \mu \end{Bmatrix} = \begin{Bmatrix} F \\ 0 \end{Bmatrix} \tag{13}$$

where, Θ is the damping matrix and F is the external load vector. The system is symmetric, frequency dependent and full. Now, Eq. (13) is solved for U and μ.

The acoustic radiation impedance matrix is defined as (Atalla and Sgard, 2015):

$$Z(\omega) = -j\rho\omega CD(\omega)^{-1}C^{T} \tag{14}$$

The sound power radiated (W_{rad}) by the vibrating plate is given by (Atalla and Sgard, 2015):

$$W_{rad} = \frac{\omega^2}{2}\left\langle U^{*}\right\rangle \text{real}[Z(\omega)]\left\{U\right\} \tag{15}$$

The radiated sound power level is expressed as:

$$\text{Sound Power Level} = 10 \times \log\left(\frac{W_{rad}}{W_{ref}}\right) \tag{16}$$

where, W_{ref} is the reference power and in the present analysis it is taken to be equal to 10^{-12} W.

The normal mean square velocity ($\left\langle v_n^2\right\rangle$) on the surface S can be written as (Atalla and Sgard, 2015):

$$\left\langle v_n^2\right\rangle(\omega) = \frac{1}{2S}\int_S \left|V_n^2\right| dS \tag{17}$$

The radiation efficiency (Ω) is a measure of the ability of the structure to radiate sound and is defined as (Atalla and Sgard, 2015)**:**

$$\Omega = \frac{W_{rad}}{\rho c S\left\langle v_n^2\right\rangle} \tag{18}$$

The sound pressure level (SPL) at a field point is given by:

$$\text{SPL}=20 \times \log\left(\frac{p}{p_{ref}}\right) \tag{19}$$

where p is the pressure at the field point and p_{ref} is the reference pressure equal to 20 μPa .

3 METHODOLOGY

The following steps are followed to obtain the coupled vibro-acoustic response of a vibrating flat panel:

1. The flat panel model is developed in ANSYS (in framework of FSDT mid-plane kinematics) using APDL code. The Shell 281 iso-parametric element from ANSYS library is used to discretize the model.

2. The modal analysis is performed after imposing appropriate support conditions and the natural frequencies and the mode shapes are obtained. The various support conditions considered in the present analysis to reduce the number of unknowns are as follows:
   (a) All edges clamped boundary condition (*CCCC*):
   $u_0 = v_0 = w_0 = \theta_x = \theta_y = \theta_z = 0$ at $x = 0$ and a; $y = 0$ and b.
   (b) All edges simply supported boundary condition (*SSSS*):
   $v_0 = w_0 = \theta_y = \theta_z = 0$ at $x = 0$ and a; $u_0 = w_0 = \theta_x = \theta_z = 0$ at $y = 0$ and b.
   (c) One edge clamped and others free condition (*CFFF*):
   $u_0 = v_0 = w_0 = \theta_x = \theta_y = \theta_z = 0$ at $x = 0$ only.
   (d) All edges hinged boundary condition (*HHHH*)
   $u_0 = v_0 = w_0 = \theta_y = \theta_z = 0$ at $x = 0$ and a; $u_0 = v_0 = w_0 = \theta_x = \theta_z = 0$ at $y = 0$ and b.
   (e) All edges free boundary condition (*FFFF*)
   $u_0 = v_0 = w_0 = \theta_x = \theta_y = \theta_z \neq 0$ at $x = 0$ and a; $y = 0$ and b.
3. The ANSYS results file (*.rst* extension) containing the modal data, as obtained in step 2, is imported into LMS Virtual.Lab environment for computing the acoustic response (Siemens LMS Virtual.Lab 13.5., Online help manual, 2015).
4. In LMS Virtual.Lab, an indirect BEM approach is adopted for obtaining the coupled responses. The loads are attached to the appropriate nodes, a field mesh (representing the microphone locations) is defined for obtaining the acoustic responses and the problem is solved.
5. The results for radiated sound power, radiation efficiency, mean square velocity and sound pressure at the field point are exported for further analysis.

The presently computed frequency responses and radiated sound power values are compared with those of the published numerical results. In addition, the numerically obtained values of the natural frequencies at different modes and the SPLs are compared with the present experimental results. The detailed experimental plan is depicted in the following section.

4 EXPERIMENTAL ANALYSIS

In order to obtain the free vibration (modal analysis) and acoustic responses of laminated composite flat panels, a lab scale experimental set-up has been developed at National Institute of Technology Rourkela (NIT, Rourkela), Odisha, India. For the experimentation purpose, two different laminated composites namely, six layered woven $[0^o/90^o]_3$ glass/epoxy and four layered symmetric angle-ply $[\pm 45^o]_s$ carbon/epoxy plates are fabricated using conventional hand lay-up technique. In order to obtain their mechanical properties, specimens are prepared in accordance with ASTM standard (D790) and a tensile test has been performed using the universal testing machine (UTM-INSTRON 1195) available at NIT, Rourkela, Odisha, India. The dimensions, lay-up scheme and material properties of the plates used for the experimental analysis are listed in Table 1.

Parameters	Glass/epoxy (Material: M1)	Carbon/epoxy (Material: M2)
Lamination Scheme	$[0°/90°]_3$	$[\pm 45°]_s$
a	0.15 m	0.15 m
b	0.15 m	0.15 m
h	0.002 m	0.00375 m
E_1	7.205×10^9 Pa	6.469×10^9 Pa
$E_2 = E_3$	6.327×10^9 Pa	5.626×10^9 Pa
$\nu_{12} = \nu_{23} = \nu_{13}$	0.17	0.3
$G_{12} = G_{13}$	2.8×10^9 Pa	2.05×10^9 Pa
G_{23}	1.4×10^9 Pa	1.025×10^9 Pa
ρ	1420.05 kgm^{-3}	1388 kgm^{-3}

Table 1: Material properties of glass/epoxy and carbon/epoxy laminated composite plates used for the experimental analysis.

Figure 3 depicts the present experimental set-up used for recording the natural frequencies and SPLs of the vibrating plate under cantilever (*CFFF*) support condition. The plate (1) is clamped along one edge using the fixture (2). The impact hammer (3) is used to excite the plate at a particular location on the plate, the signals generated are captured by the accelerometer (4), and the pressure in the surround medium is recorded by microphone (5). The accelerometer and the microphone are interfaced with LABVIEW through PXIe-1071 (6) that receives analogue voltage signal, uses an inbuilt AD (analogue to digital) converter to transform it into the digital signal form. Further, the digital signal is processed through LABVIEW software. The block diagram of the circuit designed in LABVIEW to process the signals is presented in Figure 4. The signal received from the microphone as well as the accelerometer is in the time domain. The sound pressure data from the microphone is first filtered and subsequently transformed into frequency domain by applying Fourier transform. Similarly, the acceleration response from the accelerometer is converted to frequency spectrum. This transformation is necessary to view the vibro-acoustic response of the system as a function of excitation frequency.

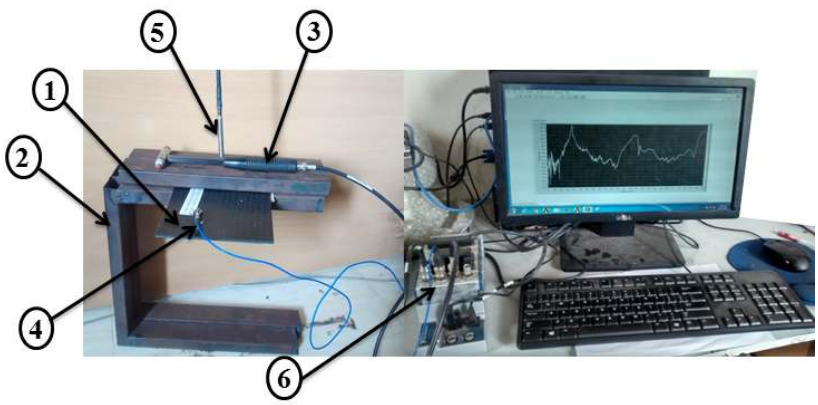

Figure 3: Experimental set-up for measuring natural frequencies and SPL of cantilever laminated composite flat panels: (1). Laminated composite plate, (2). Fixture, (3). Impact hammer, (4). Accelerometer, (5). Microphone, (6). NI PXIe 1071.

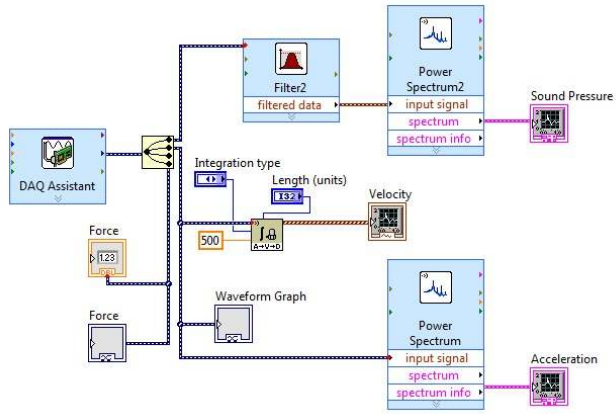

Figure 4: Diagram of circuit designed in *LABVIEW* to record vibration and acoustic response of laminated flat panels.

5 RESULTS AND DISCUSSION

The free vibration and acoustic responses of the laminated composite flat panels are computed using the proposed scheme (ANSYS and FEM/BEM approach using LMS Virtual.Lab). The efficacy and the accuracy of the present approach have been established through the convergence test and subsequent validation with available numerical and present experimentally obtained results. The effect of various structural parameters namely, thickness ratio (a/h), aspect ratio (a/b), modular ratio (E_1/E_2) and lamination scheme on the acoustic response parameters (SPL and radiated sound power) of the laminated composite flat panel for four different boundary conditions (*CCCC*, *HHHH*, *SSSS*, and *CFFF*) have been investigated using the present scheme. In the parametric study, the carbon/epoxy composite material properties, as provided in Table 2, have been utilized for the computational purpose. The panel structure is considered to be excited by a harmonic point load of 1N on the plate surface at a location bearing the coordinates ($0.25\times a$, $0.25\times b$, 0) w.r.t the coordinate system shown in Figure 1. The sound pressure level (SPL) is computed at a point in the surrounding medium lying 1m vertically above the excitation point. A modal damping of 1% has been considered throughout the analysis.

Carbon/epoxy (Material: M3)	
E_1	1.725×10^{11} Pa
$E_2 = E_3$	6.9×10^{9} Pa
$\nu_{12} = \nu_{23} = \nu_{13}$	0.25
$G_{12} = G_{13}$	3.45×10^{9} Pa
G_{23}	$0.5\times G_{12}$
ρ	1600 kgm^{-3}

Table 2: Material properties of Carbon/epoxy composite (Park et al., 2003).

5.1 Convergence and Validation Studies

As a very first step, the convergence behaviour of the present simulation model has been checked by computing the natural frequencies for different mesh divisions and simultaneously comparing them

with the available numerical data. Further, the present results are also compared with the experimentally obtained values. For the validation of the acoustic parameters, the radiated sound power of a vibrating composite plate is computed using the present scheme and compared with the existing results. Also, in order to build more confidence on the present scheme, the sound pressure levels (SPLs) at a point in the medium are obtained experimentally and compared with those computed numerically via the present approach.

5.1.1 Convergence and Validation of Natural Frequencies

In this section, the convergence behaviour and the validation for the free vibration responses computed using the present simulation model has been presented by considering different examples available in open literature. An isotropic plate under clamped boundary conditions as in Jeyaraj (2010) and a simply supported 16 layered cross-ply $[0^o/90^o]_8$ laminated composite plate as taken by Wu and Huang (2013) have been considered for testing the convergence behaviour and validating the natural frequencies. The geometry and material properties used for the computation purpose are similar to the corresponding references considered. The values of the natural frequencies for first five modes are computed for different mesh sizes and presented in Table 3 and Table 4, respectively. The analogous results available in the references are also provided for the comparison purpose. It is clearly observed that the present model is converging well with mesh refinement. Also, the present values of the natural frequencies are in excellent agreement with the reference results. Based on the convergence study a (10×10) mesh has been employed to compute the responses further throughout the present analysis.

	Natural Frequency (Hz)				
Mesh Size	Mode 1	Mode 2	Mode 3	Mode 4	Mode 5
2×2	234.70	1715.70	1715.70	3176.40	3176.40
4×4	236.51	498.94	498.94	773.31	913.04
6×6	223.63	457.50	457.50	683.94	828.49
8×8	222.66	452.58	452.58	665.77	809.82
10×10	222.52	451.65	451.65	662.86	805.33
12×12	222.48	451.39	451.39	662.16	803.81
14×14	222.47	451.28	451.28	661.93	803.18
Jeyaraj (2010)	224	456	456	673	819

Table 3: Convergence and validation of natural frequencies of a clamped square isotropic plate.

	Natural Frequency (Hz)					
Mesh Size	Mode 1	Mode 2	Mode 3	Mode 4	Mode 5	Mode 6
2×2	221.10	1703.30	2615.5	2747.20	2786.80	6977.30
4×4	157.10	317.48	457.00	608.82	761.50	999.64
6×6	156.21	296.56	444.13	504.35	633.24	801.68
8×8	156.16	295.46	443.03	496.18	624.36	767.34
10×10	156.15	295.29	442.78	494.76	623.32	760.66
12×12	156.15	295.24	442.69	494.32	623.08	758.51
14×14	156.15	295.22	442.65	494.14	623.00	757.61
Wu and Huang (2015)	154	291	442	489	614	755

Table 4: Convergence and validation of natural frequencies of a simply supported rectangular laminated composite plate.

5.1.2 Experimental Validation of Natural Frequency

Experiments have been conducted to acquire the free vibration responses of six layered woven glass/epoxy plate and four layered symmetric angle-ply $[\pm 45^{o}]_{s}$ carbon/epoxy laminated plate using a lab scale experimental set-up as described in Section 4. The dimensions, lay-up scheme and material properties (M1 and M2) of the specimens are provided in Table 1. The natural frequencies are obtained for first five modes under *CFFF* boundary condition and shown in Table 5 along with the results computed using the current simulation model. It is evident from both the convergence and comparison study that the present numerical results are in good agreement with the established numerical values and present experimental results as well. The slight differences between the numerical and the experimentally obtained values can be attributed to the limitation in applying the perfect displacement boundary conditions on the plate as it is very difficult to replicate the exact conditions for multiple tests of the same specimen.

Mode No.	Natural Frequency (Hz)					
	Material: M1			Material: M2		
	Present experimental	Present numerical	% diff.	Present experimental	Present numerical	% diff.
1	28	29.431	4.862	62.5	56.038	-11.531
2	68	79.319	14.270	152	140.29	-8.347
3	164	183.4	10.578	378	340.2	-11.111
4	234	236.26	0.957	485	441.53	-9.845
5	267	278.97	4.291	561	503.23	-11.480

Table 5: Experimental validations of the natural frequencies of six layered woven glass/epoxy composite flat panel (M1) and four layered symmetric angle-ply carbon/epoxy flat panel (M2) under *CFFF* boundary condition.

5.1.3 Validation of the Acoustic Parameters

From the discussion in the previous sections, it is clear that the present simulation model yields valid results for the free vibrations response of the vibrating laminated composite flat panels under different boundary conditions. In this section, the mode shapes for each natural frequency of vibration are extracted and used to compute the acoustic responses for the vibrating composite flat panels using coupled FEM/BEM approach in LMS Virtual.Lab environment. The sound power radiated by the plate and the SPL at a particular location in the surrounding medium are obtained to analyse the sound radiation characteristic. Initially, the radiated sound power values computed using the present scheme is compared with those reported in open literature. Then, the corresponding values of SPLs are also validated with the present experimentally obtained values using the lab-scale experimental set-up.

5.1.3.1 Validation of the Radiated Sound Power

A square isotropic (mild steel) plate of side 1m and clamped along its all four edges as in Jeyaraj (2010) has been chosen for the numerical validation of the radiated sound power. In the present analysis two excitation cases (same as in the reference) of harmonic point load of 1N are considered

and referred as Excitation-1 and Excitation-2 for the load acting at the central node and at a location (0.7m, 0.7m, 0) with reference to Figure 1, respectively. The sound power radiated by the plate is computed using the present formulation for the above two cases and shown in Figure 5 (a) and (b), respectively for the comparison with the reference values. It can be clearly seen that the sound power level computed using the present scheme match very well with the results reported in the reference over the entire range of frequencies considered.

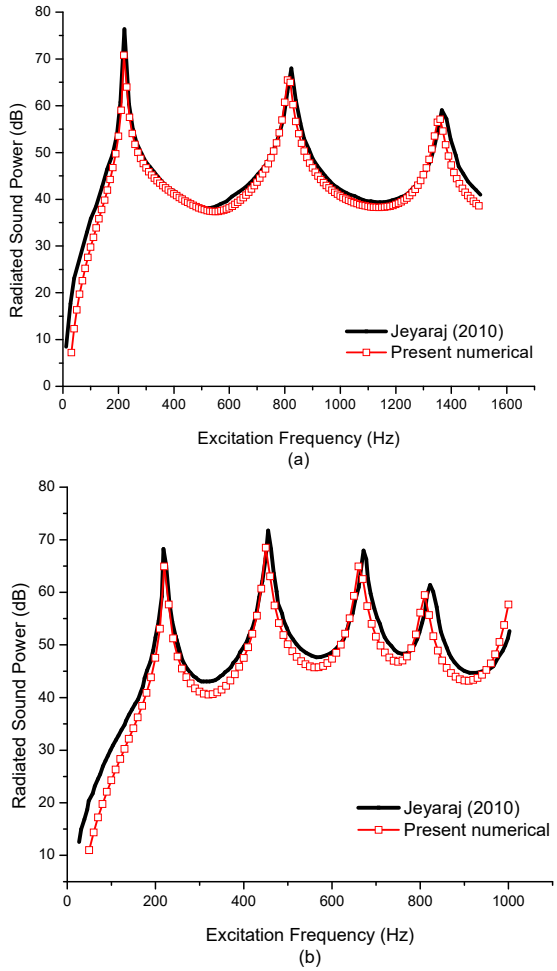

Figure 5: Validation study of sound power level (a) Excitation type 1, (b) Excitation type 2.

5.1.3.2 Experimental Validation of Sound Pressure Level

Laminated composite flat panels of M1 and M2 materials, as in Table 1, under *CFFF* boundary conditions are considered for experimentally (described in Section 4) determining the SPL at a point in the surrounding medium. The panels are excited by a 1N harmonic point load at the central node on the free edge opposite to the clamped edge and the SPL is measured at a distance of 0.1m above the central point of the plate. With similar considerations, the SPL values are computed using the present numerical model and validated by comparing with those experimentally ob-

tained data. The comparison of the experimental and numerical results for SPL of the vibrating flat panel with M1 and M2 material properties are shown in Figure 6 (a) and (b), respectively. It is observed that in both the cases the present numerical values of SPL follow closely the experimental results (including the occurrence of peaks and depressions) up to the excitation frequency of 200 Hz, after which slight deviation is noticed. The reason for the deviation may be due to the limitations in applying displacement boundary condition on the structure and the absence of anechoic chamber during experimentation. It is also worthy to mention that the present numerical results have been computed by considering a modal damping ratio of 1% (which is the usual case for laminated composite structures) and that may not agree exactly with the damping occurring in the plates used for experimentation.

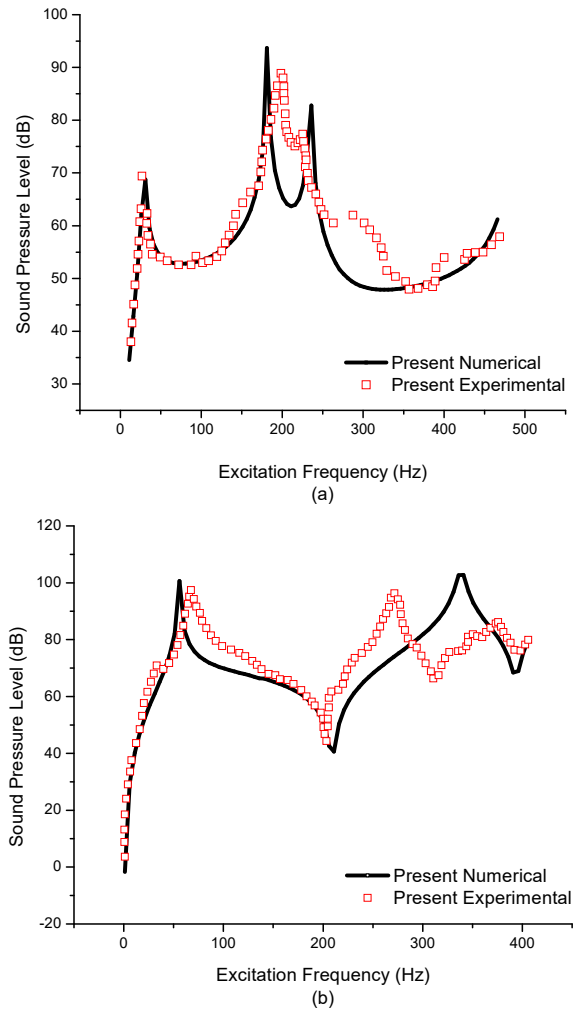

Figure 6: Experimental validation study of SPLs for the vibrating plate structure (a) six layered cantilever woven glass/epoxy flat panel and (b) four layered cantilever angle-ply laminated carbon/epoxy flat panel.

5.2.1 Influence of Structural Parameters on Sound Pressure Level and Radiated Sound Power

5.2.1.1 Influence of the Thickness Ratio

The influence of thickness ratio on the acoustic radiation behaviour of a four layered clamped symmetric cross-ply $[0^o/90^o]_s$ laminated composite flat panel is investigated in this example. The plate dimensions are taken as $a = 0.4$ m, $b = 0.3$ m and h is varied such that $a/h = 5$, 10, 40, 60, and 100. The laminated composite plate has two coincidence frequencies, which are a function of plate thickness and Young's moduli of the material (Ohlrich and Hugin, 2004). The coincidence frequencies in Hz for each thickness value are (75.6, 378.03), (151.2, 756), (604.85, 3024.26), (907.28, 4536.4) and (1512.13, 7560.6), respectively. Therefore, a frequency range of 0-10,000 Hz is considered to observe the sonic and subsonic behaviour of plates. The variation of the radiation efficiency and the radiated sound power with the excitation frequency for different values of thickness ratio is shown in Figure 7 (a) and (b), respectively. It can be observed that the average radiation efficiency increases with increasing thickness ratio. For the thinnest plate (a/h=100), radiation efficiency is more as compared to the others due to reduced stiffness. This leads to shifting of natural modes of vibration to lower frequencies and higher coincidence frequencies in the considered frequency range. Also, it is worthy to note that the radiation efficiency exceeds 1 close to the first coincidence frequency and asymptotically decreases to 1 after the second coincidence frequency in most of the cases. The radiated sound power increases with increasing plate thickness ratio. A similar trend is observed for the sound pressure level in near and far-fields for modes (1,1) and (2,1) of the plates as shown in the SPL directivity plots in Figure 7(c) and (d), respectively.

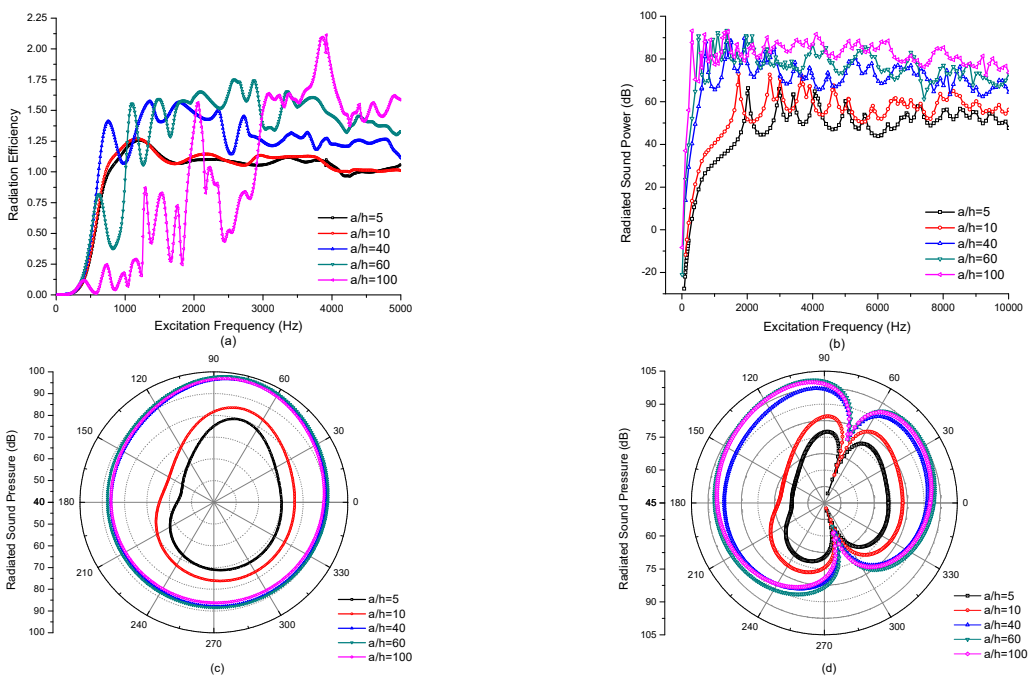

Figure 7: Influence of thickness ratio on the (a) Radiation efficiency; (b) Radiated sound power; (c) Sound pressure level directivity for mode (1,1) and (d) Sound pressure level directivity for mode (2,1) of the laminated composite flat panel (*CCCC*, four layered symmetric cross-ply, $(0^o/90^o)_s$).

5.2.1.2 Influence of the Aspect Ratio

To study the influence of aspect ratio (a/b) on the SPL and the sound power radiated in the surrounding medium, a four layered anti-symmetric cross-ply $[\pm 45^o]_2$ laminated composite flat panel under *HHHH* support condition has been considered. For the computation purpose the geometry of the panel is taken as $a = 0.4$ m, $h = 0.01$ m fixed and b is varied such that $(a/b) = 0.5$, 1, 1.5, 2, 2.5. The plate has the same coincidence frequencies (604.85, 3024.27) Hz for all of the aspect ratios. The plates' mass and stiffness is affected by changing the aspect ratio leading to a change in the vibration energy of the plate. The radiation efficiency generally decreases with increasing aspect ratio; a/b=0.5 case causes the maximum acoustic radiation onto the second coincidence frequency and the same can be observed from Figure 8 (a). The average sound power level follows an increasing trend with decreasing aspect ratio with the resonance peaks shifting to lower frequencies as shown in Figure 8(b). It is also worthy to note that the radiation efficiency exceeds unity indicating that radiated acoustic power is more than the vibration energy of the plates.

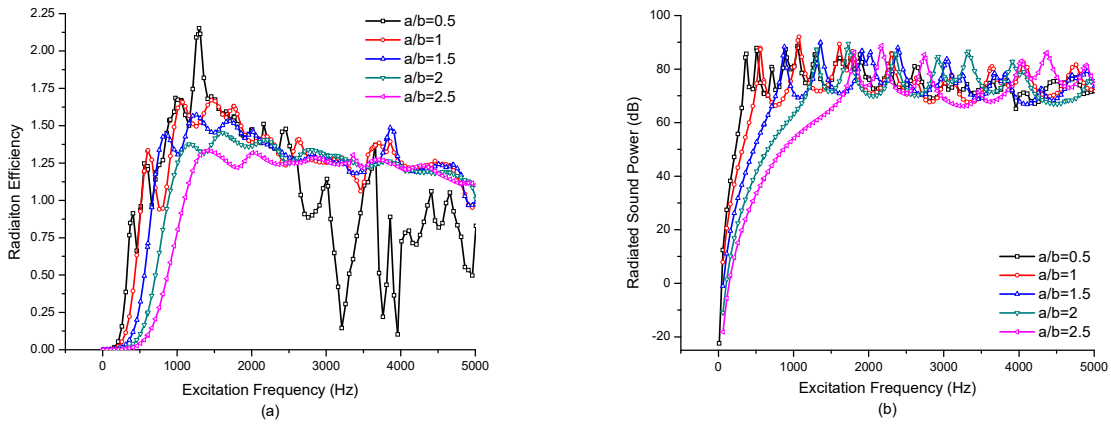

Figure 8: Influence of aspect ratio on the (a) Radiation efficiency and (b) Radiated sound power of the laminated composite flat panel (*HHHH* four layered anti-symmetric cross-ply, $[45^o/\text{-}45^o]_2$).

5.2.1.3 Influence of Modular Ratio

The effect of modular ratio on the acoustic emissions from a vibrating simply supported anti-symmetric angle-ply $[\pm 45^o]_2$ rectangular laminated composite flat panel ($a = 0.4$ m, $b = 0.3$ m, and $h = 0.01$ m) has been analysed. The radiation efficiency and the radiated sound power is obtained for $E_1/E_2 = 5$, 10, 15, 20, and 25 configurations. The first coincidence frequency is the same equal to 604.85 Hz for all configurations and the second coincidence frequencies are 1352.5 Hz, 1912.7 Hz, 2342.6 Hz, 2705 Hz, and 3204.3 Hz for each configuration, respectively. It is interesting to note that the first natural frequencies of the configurations are very close to the first coincidence frequency. It can clearly be observed from Fig. 9 that the radiation efficiency and radiated sound power are not affected greatly by the varying modular ratio. It is can be seen that for every value of modular ratio the curves closely follow each other over the entire frequency range with the peaks and valleys oc-

curring at almost same values of excitation frequency. The radiation efficiency crosses unity around the first natural frequency for all configurations of modular ratio and approaches unity after crossing the maximum value of second coincidence frequency.

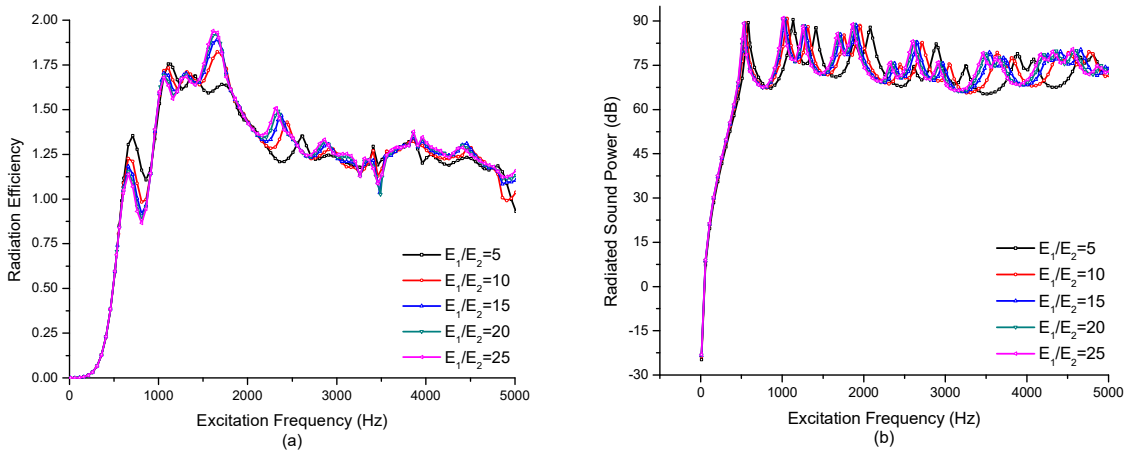

Figure 9: Influence of modular ratio on the (a) Radiation efficiency and (b) Radiated sound power of the laminated composite flat panel (*SSSS* 4-layered anti-symmetric angle-ply, $[45^o/\text{-}45^o]_2$).

5.2.1.4 Influence of Lay-Up Scheme

It is well known that, the lay-up scheme of any laminated composite structure significantly governs the stiffness and thus affects the vibration and sound radiation behaviour greatly. The effect of lamination scheme on the sound radiation characteristics of a vibrating laminated composite flat panel ($a = 0.4$ m, $b = 0.3$ m, and $h = 0.01$ m) under *CFFF* support condition for different layup schemes. The SPL is obtained at a point 1m directly above the excitation location on the plate. It is observed from Figure 10 that the SPL at the field point and the radiated sound power is greatly influenced by the lay-up scheme of the vibrating plate. It is worthy to note that, over the entire frequency range the plate exhibits similar sound radiation behaviour for both the symmetric $[45^o/\text{-}45^o]_s$ and anti-symmetric $[45^o/\text{-}45^o]_2$ angle-ply lamination cases. However, there is a considerable difference between the sound radiation characteristics of symmetric $[0^o/90^o]_s$ and anti-symmetric $[0^o/90^o]_2$ cross-ply laminations. It can also be seen that the peaks occur at higher frequencies for cross-ply laminations in comparison to the angle-ply schemes. However, the average SPL is lower for cross ply configuration compared to the angle ply configuration with the minimum value for $[0^o/90^o]_2$ case as shown in Table 6.

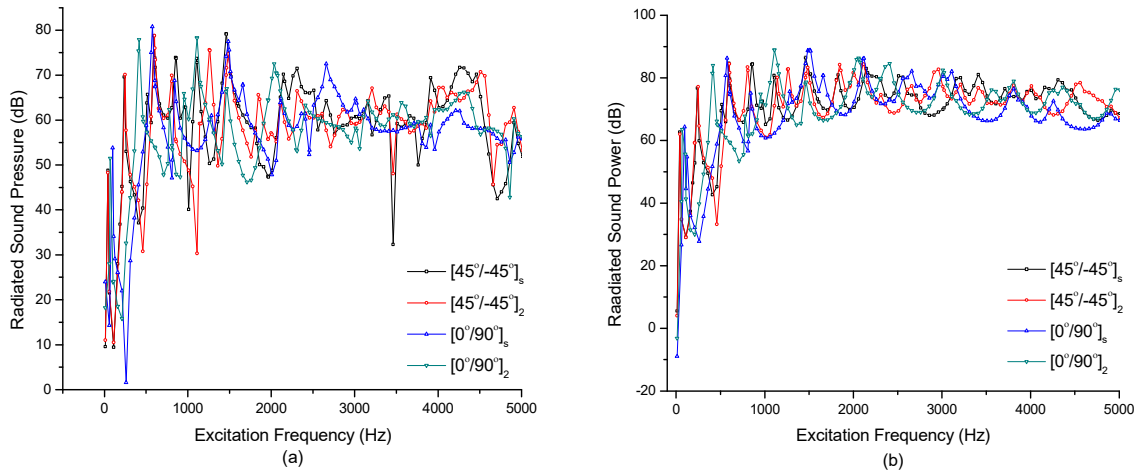

Figure 10: Influence of lay-up scheme on the (a) Radiated sound pressure and (b) Radiated sound power of the laminated composite flat panel (*CFFF* 4-layered).

Lay-up	$[45^o/-45^o]_s$	$[45^o/-45^o]_2$	$[0^o/90^o]_s$	$[0^o/90^o]_2$
Average SPL	60.125	59.424	58.496	58.364

Table 6: SPL values for different lay-ups.

5.2.1.5 Influence of Support Conditions

The number of constraints on the degrees of freedom at the support plays a significant role on the stiffness characteristics of any structure/structural component. The stiffness increases as the number of constraints increases or the degree of freedom decreases and this may have a substantial effect on the sound radiation characteristic of the structure. In this section, an anti-symmetric angle-ply $[45^o/-45^o]_2$ rectangular (0.4 m×0.3 m×0.01 m) laminated composite flat panel has been considered for analysis. The first and the second coincidence frequencies are (604.85, 3024.27) Hz. The *FFFF* and *CFFF* configurations have many resonances before the first coincidence frequency. Therefore, the sound pressure level at a field point 1 m directly above the excitation location on the plate and the radiated sound power is computed for four different support conditions (*FFFF*, *CCCC*, *SSSS* and *CFFF*) in the frequency range 0-1000 Hz and presented in Figure 11 (a) and (b), respectively. The influence of the number of constraints at the support is well reflected in the results. It is observed that, over low excitation frequency range i.e., upto 1000 Hz, the sound power radiated from the vibrating plate decrease with increasing number of constraints at the support. However, the average sound power is the least for *FFFF* case followed in the increasing order by *CFFF*, *CCCC* and *SSSS* and the same can be observed from the plot of sound power level for frequency range 0-5000 Hz, as shown in Figure 11 (c).

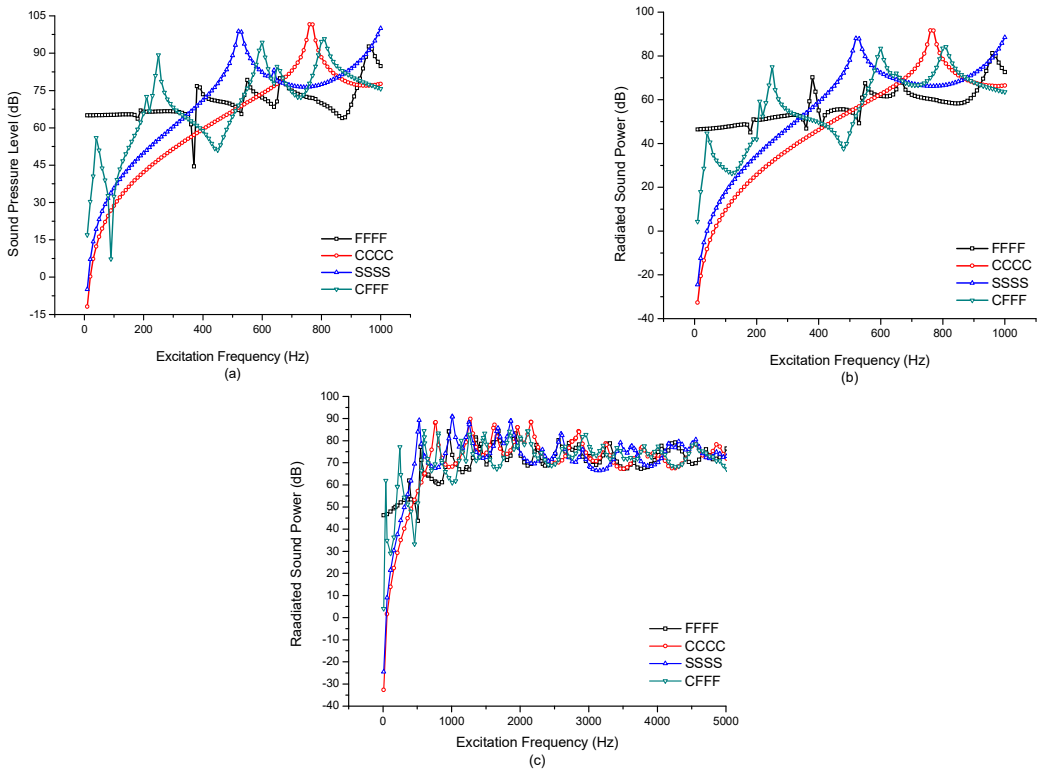

Figure 11: Influence of support condition on the (a) Sound pressure level at field point (0-1000 Hz); (b) Radiated sound power (0-1000 Hz) and (c) Radiated sound power of the laminated composite flat panel (0-5000 Hz)(4-layered anti-symmetric angle-ply $[45°/-45°]_2$).

5.2.2 Case Study: Vibro-Acoustic Response from Laminated Flat Panels of Various Composite Materials

In this section, a case study has been presented to compare the vibro-acoustic behaviour of the laminated flat panel of different composite materials those are widely used in their key areas of application. Four different composite materials namely, graphite-epoxy, boron-epoxy, kevlar-epoxy and glass-epoxy are considered for the present analysis and their properties are listed in Table 7.

Properties	Graphite-epoxy (Kumar et al., 2010)	Boron-epoxy (Kumar et al., 2010)	Kevlar-epoxy (Kumar et al., 2010)	Glass-epoxy (Daneshjou et al., 2007)
E_1	1.37×10^{11} Pa	2.04×10^{11} Pa	76×10^{9} Pa	38.6×10^{9} Pa
$E_2 = E_3$	8.9×10^{9} Pa	18.3×10^{9} Pa	5.5×10^{9} Pa	8.2×10^{9} Pa
$\nu_{12} = \nu_{23} = \nu_{13}$	0.28	0.23	0.23	0.26
$G_{12} = G_{13}$	7.1×10^{9} Pa	5.5×10^{9} Pa	2.4×10^{9} Pa	4.2×10^{9} Pa
G_{23}	$0.5\times G_{12}$	$0.5\times G_{12}$	$0.5\times G_{12}$	$0.5\times G_{12}$
ρ	1600 kgm^{-3}	2000 kgm^{-3}	1460 kgm^{-3}	1900 kgm^{-3}

Table 7: Composite material properties of various laminated flat panels used for computation in the case study.

For the computation purpose a simply supported rectangular (0.5 m × 0.5 m × 0.02 m), anti-symmetric cross-ply $[0°/90°]_2$ laminated composite flat panel subjected to unit harmonic point load at

(0.125 m, 0.125 m) from the lower left corner is considered. The SPL directivity pattern for modes (1,1) and (2,1), the radiation efficiency and the radiated sound power level values are computed for various composite materials using the present scheme and shown in Figure 12 (a)-(d), respectively. In general, the RMS values of a vibrating structure are considered to judge its suitability for a particular application. As evident from Figure 12 (a), (b), the SPL is the lowest for glass-epoxy corresponding to both of the modes. Also, the directivity patterns are of monopole and dipole nature in accordance with the mode shapes of (1,1) and (2,1) modes, respectively. The frequencies of first few resonance modes of glass-epoxy and kevlar-epoxy are lesser than the first coincidence frequencies which are around 700.2 Hz and 437.46 Hz, respectively. The radiation efficiencies of each material cross unity at the corresponding first coincidence frequency thereafter, following an asymptotic decrement to unity. The radiation efficiency curves for kevlar-epoxy and glass-epoxy are more fluctuating as compared to boron-epoxy and graphite-epoxy over the frequency range under consideration. This is due to the fact that, for glass-epoxy and kevlar-epoxy the longitudinal Young's modulus (E_1) is relatively low, which leads to reduced stiffness. The same can also be observed from the plot of radiated sound power shown in Figure 12 (d). This may also be attributed to the higher values of E_1/G_{12} ratio for these materials (kevlar-epoxy and glass-epoxy) as compared to the relatively stiffer materials (graphite-epoxy and boron-epoxy). However, the behaviour of graphite- epoxy and boron-epoxy is identical throughout the frequency range under consideration and the same can be observed from the radiation efficiency and sound power level plots shown in Figure 12 (c) and (d), respectively.

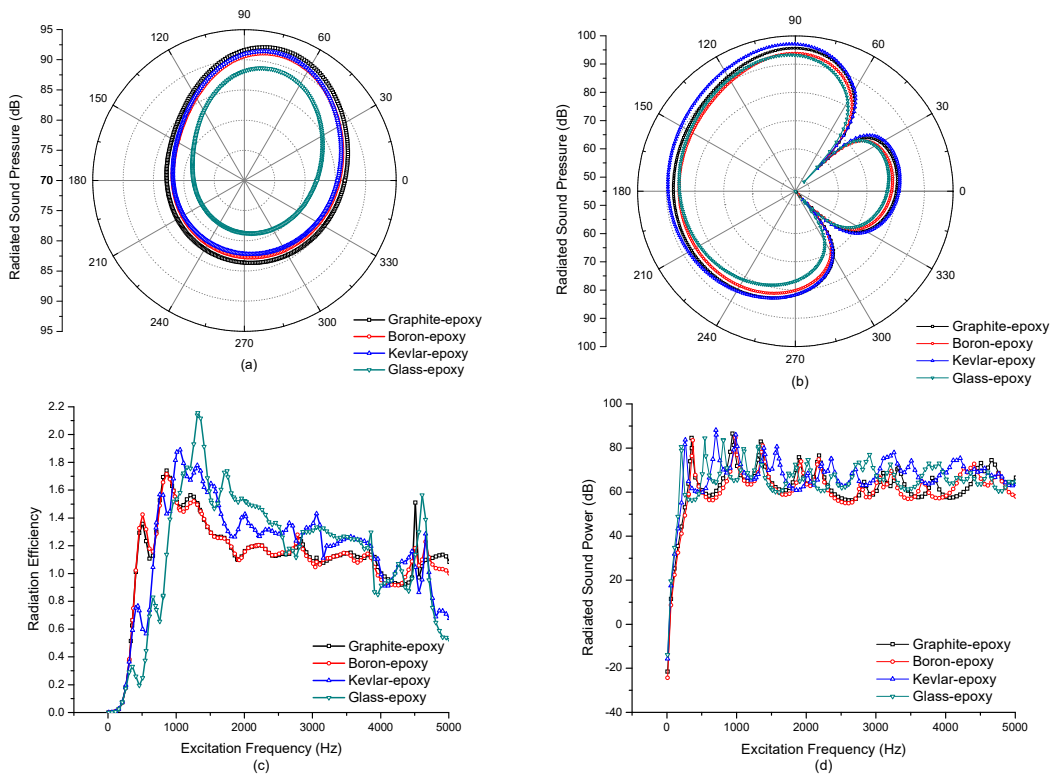

Figure 12: Comparison of acoustic responses from the laminated flat panel of different composite materials (a) Sound pressure level directivity for mode (1,1); (b) Sound pressure level directivity for mode (2,1); (b) Radiation efficiency and (d) Radiated sound power.

6 CONCLUSIONS

The vibration and acoustic responses of un-baffled laminated composite flat panels excited by harmonic point load and under various support conditions have been investigated in this article. The natural frequencies are computed with the help of a simulation model developed in ANSYS using APDL code. The results of modal analysis are exported to LMS Virtual.Lab environment, wherein the coupled vibro-acoustic responses of the vibrating panel are obtained using an indirect BEM. First, the free vibration responses obtained using the present simulation model are compared with the published numerical results and present experimentally determined values as well to test its validity. For the experimental analysis, the laminated composite plates were manufactured by hand lay-up technique and necessary steps were taken to ensure uniform thickness variation. The cantilever boundary condition was imposed on the plate by sandwiching it between the two bars and fully tightening them with the help of the nuts and bolts to closely match the corresponding constraints applied to the numerical model. Then, the ability and correctness of the present FEM/BEM scheme to compute the acoustic responses have been established by comparing the present responses with the numerical results available in open literature. The results are also compared with those obtained experimentally using the in-house experimental set-up. Finally, an extensive study has been performed to investigate the effect of geometrical parameters, support conditions and material properties on the sound radiation characteristics of laminated composite flat panels. The sound pressure directivity in the medium, radiation efficiency and the radiated sound power of the vibrating plate is chosen as the acoustic response indicators. It is observed that the sound radiation behaviour of the laminated composite plate is greatly influenced by the lay-up scheme and number of constraints at the support. It is also noted that the acoustic responses increase with thickness ratio, decrease with aspect ratio and insignificantly affected by varying modular ratio. All materials exhibit dissimilar vibro-acoustic behaviour however, the sound radiation characteristics of the graphite- epoxy and boron-epoxy laminated plates are very close to each other. Among all the materials utilised for the present study, the sound pressure level for glass-epoxy is the least.

Acknowledgement

The authors of the article are thankful to Prof. Vishesh Ranjan Kar, Department of Design and Automation, School of Mechanical Engineering, VIT University, Vellore 632014, TN, India for providing access to LMS Virtual.Lab including a few more specific facilities.

References

Atalla, N., Nicolas, J., Gauthier, C., (1996). Acoustic radiation of an unbaffled vibrating plate with general elastic boundary conditions. Journal of Acoustical Society of America 99.

Atalla, N., Sgard, F., (2015). Finite element and boundary methods in structural acoustics and vibration, CRC Press, Taylor and Francis Group, Boca Raton, Florida, USA.

Cook, R. D., Malkus, D. S., Plesha, M. E., (2000). Concepts and applications of finite element analysis, 3rd edition, John Willy and Sons, Singapore.

Daneshjou, K., Nouri, A., Talebitooti, R., (2007). Sound transmission through laminated composite cylindrical shells using analytical model. Archives of Applied Mechanics 77:363–379.

Everstine, G. C., Henderson, F. M., (1990). Coupled finite element/boundary element approach for fluid–structure interaction, Journal of Acoustical Society of America 87:1938.

Holmstrom, F., (2001). Structure-acoustic analysis using BEM/FEM; Implementation in MATLAB, M.S. thesis, Lund University, Sweden.

Huang, M., Ma, X. Q., Sakiyama, T., Matuda, H., Morita, C., (2005). Free vibration analysis of orthotropic rectangular plates with variable thickness and general boundary conditions. Journal of Sound and Vibration 288:931–955.

Jeyaraj, P., (2010). Vibro-acoustic behavior of an isotropic plate with arbitrarily varying thickness. European Journal of Mechanics - A/Solids 29:1088–1094.

Jeyaraj, P., Ganesan, N., Padmanabhan, C., (2009). Vibration and acoustic response of a composite plate with inherent material damping in a thermal environment. Journal of Sound and Vibration 320:322–338.

Jeyaraj, P., Padmanabhan, C., Ganesan, N., (2008). Vibration and Acoustic Response of an Isotropic Plate in a Thermal Environment. Journal of Vibration and Acoustics 130: 051005.

Kumar , B. R., Ganesan, N., Sethuraman, R., (2009). Vibro-acoustic analysis of functionally graded elliptic disc under thermal environment. Mechanics of Advanced Materials and Structures. 16:160–172.

Kumar, B. R., Ganesan, N., Sethuraman, R., (2010). Vibro-acoustic analysis of composite elliptic disc with various orthotropic properties. Journal of Composite Materials 44:1179–1200.

Li, S., Li, X., (2008). The effects of distributed masses on acoustic radiation behavior of plates, Applied Acoustics 69:272–279.

Nowak, L. J., Zieliński, T. G., (2015). Determination of the Free-Field Acoustic Radiation Characteristics of the Vibrating Plate Structures With Arbitrary Boundary Conditions. Journal of Vibration and Acoustics 137:051001–1–051001–8.

Ohlrich, M., Hugin, C.T., (2004). On the influence of boundary constraints and angled baffle arrangements on sound radiation from rectangular plates. Journal of Sound and Vibration 277:405–418.

Park, J., Mongeau, L., Siegmund, T., (2003). Influence of support properties on the sound radiated from the vibrations of rectangular plates. Journal of Sound and Vibration 264:775–794.

Petrone, G., D'Alessandro, V., Franco, F., S. de Rosa, (2014). Numerical and experimental investigations on the acoustic power radiated by Aluminium Foam Sandwich panels. Composite Structures 118:170–177.

Putra, A., Thompson, D. J., (2010). Sound radiation from rectangular baffled and unbaffled plates. Applied Acoustics 71:1113–1125.

Qiao, Y., Huang, Q., (2007). The effect of boundary conditions on sound loudness radiated from rectangular plates, Archives of Applied Mechanics 77:21–34.

Shojaeefard, M. H., Talebitooti, R., Ahmadi, R., Gheibi, M. R., (2014). Sound Transmission across Orthotropic Cylindrical Shells Using Third-order Shear Deformation Theory. Latin American Journal of Solids and Structures 11: 2039-2072.

Siemens LMS Virtual.Lab 13.5., (2015). Online help manual.

Tournour, M., Atalla, N., (1998). Vibroacoustic behavior of an elastic box using state-of-the-art FEM–BEM approaches. Noise Control Engineering Journal 46.

Wu, J., Huang, L., (2013). Natural frequencies and acoustic radiation mode amplitudes of laminated composite plates based on the layerwise FEM. International Journal of Acoustics and Vibration 18:134–140.

Yin, X. W., Cui, H. F., (2009). Acoustic Radiation From a Laminated Composite Plate Excited by Longitudinal and Transverse Mechanical Drives. Journal of Applied Mechanics 76:044501.

Zhao, X., Geng, Q., Li, Y., (2013). Vibration and acoustic response of an orthotropic composite laminated plate in a hygroscopic environment. Journal of Acoustical Society of America 133:1433–1442.